

Analysis of signal propagation in optically coupled detectors for digital mammography. I.  
Phosphor screens

This content has been downloaded from IOPscience. Please scroll down to see the full text.

1995 Phys. Med. Biol. 40 877

(<http://iopscience.iop.org/0031-9155/40/5/011>)

View [the table of contents for this issue](#), or go to the [journal homepage](#) for more

Download details:

IP Address: 170.212.0.65

This content was downloaded on 15/07/2016 at 18:41

Please note that [terms and conditions apply](#).

## Analysis of signal propagation in optically coupled detectors for digital mammography: I. Phosphor screens

Andrew D A Maidment† and Martin J Yaffe

Departments of Medical Biophysics and Radiology, University of Toronto, and Research Division, Sunnybrook Health Science Centre, 2075 Bayview Avenue Toronto, Ontario M4N 3M5, Canada

Received 6 October 1994

**Abstract.** The angular emission of light from turbid phosphor screens has been measured and modelled. As a first approximation, turbid phosphor screens have traditionally been modelled as Lambertian sources; however, Giakoumakis *et al* have previously shown that light emission from turbid phosphor screens is in fact more forward peaked. In this article, we extend the theory of Giakoumakis to include turbid phosphor screens that incorporate a transparent overcoat. The refractive index of the optical coupling medium in contact with the overcoat is shown to have a direct effect on both light output and angular emission from the screen. It was found that simple laws of refraction adequately describe this phenomenon. To model the angular emission of light from such phosphor screens, a term was included to describe the refraction from the overcoat into the adjacent coupling medium. The data obtained are required to calculate the propagation of the signal in a digital mammography detector in which a phosphor screen is optically coupled to a charge-coupled device (CCD) image array.

### 1. Introduction

A digital radiographic imaging system is being developed at the University of Toronto for use in full-field digital mammography (Maidment *et al* 1993a). The detector, shown schematically in figure 1, consists of a mammographic phosphor screen, coupled via a fibre optic taper to a time delay integration (TDI) mode charge-coupled device (CCD) image array. The output of each CCD is digitized and transferred using direct memory access (DMA) to a computer workstation. Images are acquired by scanning the detector in one direction across the breast. In this paper, digital detectors with such optical couplings will be referred to as phosphor-optics-CCD (POC) detectors.

POC detectors can be treated as consisting of serially cascaded components which propagate x-ray, light or electron images. The signal to noise ratio (SNR) of POC detectors is determined, in part, by the efficiency with which light quanta are produced in a phosphor screen and then collected and recorded (Maidment and Yaffe 1994). Both the magnitude and angular emission of light from the phosphor screen, as well as the angular acceptance and transmission efficiency of the intervening optics, affect the optical coupling efficiency. In this paper, the former are considered. Both experimental measurements and a new model for calculating the angular emission of light from phosphor screens are described. The model is valid for turbid phosphor screens that have a protective overcoat layer. A method

† Current address: Department of Radiology, Thomas Jefferson University, 3390 Gibbon Building, 111 South 11th Street, Philadelphia, PA 19107-5098, USA.

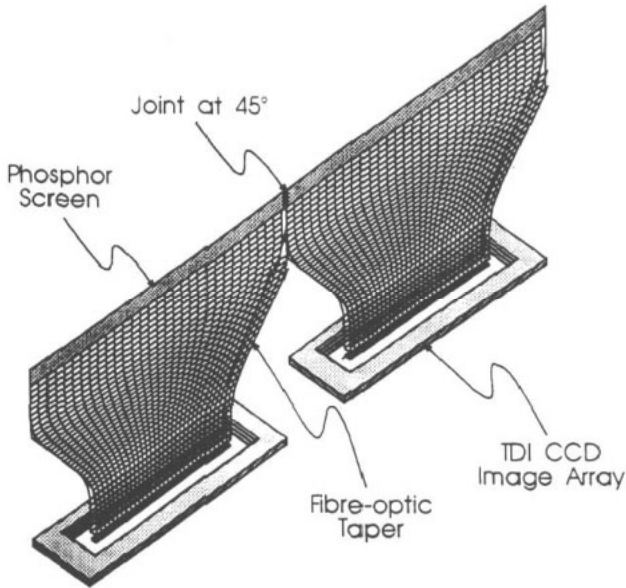


**Figure 1.** A schematic diagram of the prototype digital mammography detector, in which a phosphor screen is coupled via demagnifying fibre optic tapers to TDI CCD image arrays. To image the breast, the detector must be scanned across the breast in synchrony with the TDI operation.

for analysing the absorption of x-rays and the generation of light quanta in phosphors has been presented previously (Maidment *et al* 1993b).

Two POC detectors are shown in figure 2. Both detectors use a single optical component to convey light from the phosphor screen to the CCD image array. In figure 2(a) the optical coupling is provided by a relay lens, while in figure 2(b) a demagnifying fibre optic taper is shown. These detectors are representative of those being proposed for use in digital mammography systems (Beerlage *et al* 1986, Fritz 1989, Karellas *et al* 1992, Maidment *et al* 1993a, Nelson *et al* 1982, Sashin *et al* 1976). Fused fibre optic arrays (Kapany 1955), because of their large acceptance solid angle, have the potential to provide far greater optical coupling efficiencies than are possible with lenses. However, a phosphor screen must be in intimate contact with the fibre optic, making comparisons of the coupling efficiency of fibre optics and lenses difficult. In this paper, we consider the effect of the refractive index of the medium into which the phosphor screen is coupled. This permits the comparison of the optical coupling efficiency of lens and fibre-optically coupled POC detectors.

## 2. Theory

In POC detectors, a phosphor screen is directly coupled to a lens or fibre optic, for which propagation of light is dependent upon the angle of incidence. Thus, it is necessary to know the angular distribution of the light emitted from the phosphor screen. The angular-dependent propagation of light is illustrated in figure 3. The angular dependence of the emission of light from phosphor screens was measured experimentally as described below. Here, a model is proposed to describe this angular dependence. This model is derived from

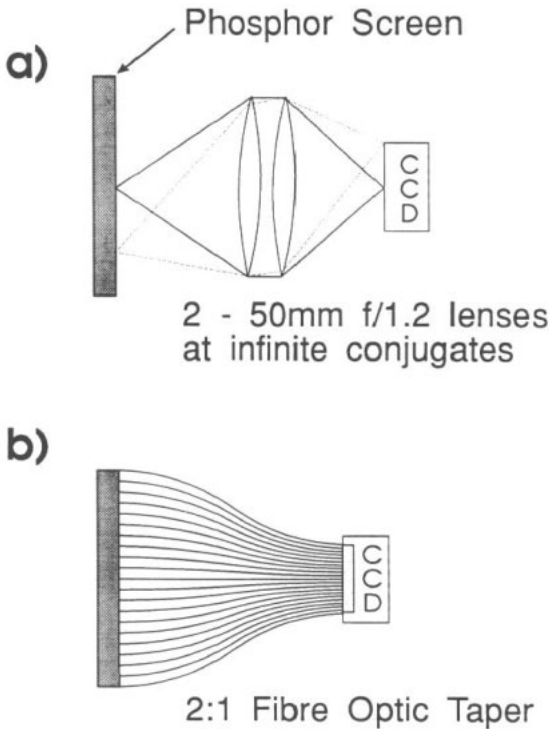


**Figure 2.** Two POC detectors are shown. In each case, a phosphor screen is optically coupled to a CCD image array. The optical coupling consists of relay lenses (a) and a fused fibre optic taper (b).

that of Giakoumakis and Miliotis (1985), and is applicable to phosphor screens that have a protective overcoat layer.

In Giakoumakis's model, a phosphor screen is divided into thin layers, as illustrated in figure 4(a). In that model, it was assumed that the angular distribution of the light generated in each layer is Lambertian, hence, the radiance is independent of angle  $\theta$ . It was also assumed that the amount of light arising from optical scattering in each layer is invariant with depth and can be linearly related to the thickness of the phosphor layer,  $dz$ , by a constant,  $\lambda$ . However, because of both the optical scattering and absorptive processes in the screen, light quanta generated at large angles to the normal of the screen surface and light quanta generated far from the screen surface are less likely to be emitted from the screen. The light emitted at the surface of the phosphor screen from the layer at  $z$  is given by (Giakoumakis and Miliotis 1985)

$$dL(\theta, z) = e^{-k_p z / \cos(\theta)} \lambda dz \tag{1}$$

where  $k_p$  is a fitted parameter related to the optical scattering and absorption properties of the phosphor material. The normalized radiance

$$L(\theta)/L(0) = [(1 - e^{-k_p t_p / \cos(\theta)}) / (1 - e^{-k_p t_p})] \cos(\theta) \tag{2}$$

has been calculated by integrating equation (1) with respect to  $z$  over the thickness of the screen,  $t_p$  (Giakoumakis and Miliotis 1985). Typically, the optical attenuation coefficient,

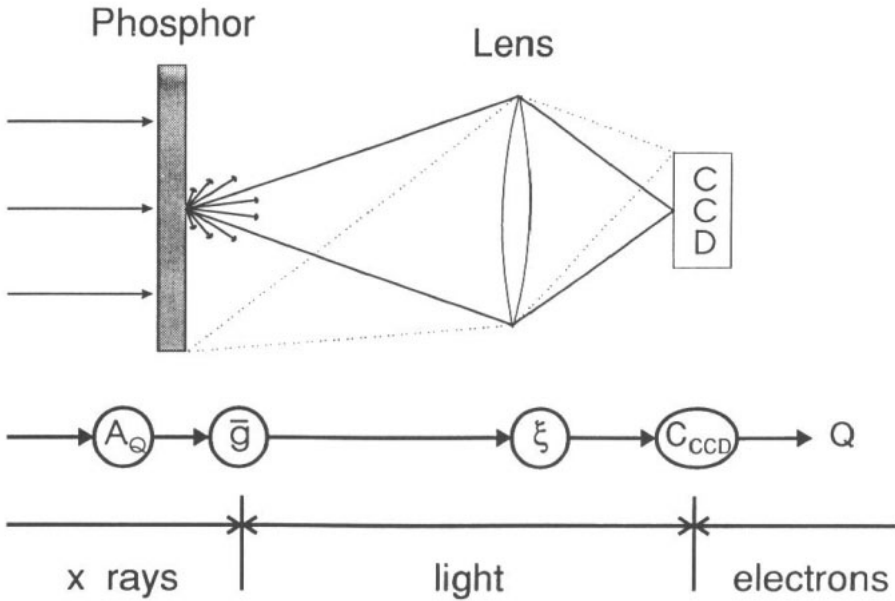


**Figure 3.** A schematic diagram of a detector in which a phosphor screen is optically coupled to a CCD. X-rays are incident on a phosphor screen with quantum interaction efficiency,  $A_Q$ , which produces  $\bar{g}$  light quanta per x-ray absorbed. These light quanta are coupled with efficiency  $\xi$  to a CCD with conversion efficiency  $C_{CCD}$  electrons per light quantum, producing a total of  $Q$  electrons.

$k_p$ , has units of inverse distance, while the screen thickness,  $t_p$ , will have units of distance, so that  $k_p t_p$  is unitless.

In commercial phosphor screens, the phosphor material is protected from abrasion by an overcoat layer, as shown in figure 4(b). To a first approximation, the overcoat can be considered to be optically flat, hence refraction from the overcoat material to the coupling medium must be considered in calculating the angular emission of light from the phosphor screen. The model of Giakoumakis may be modified by relating the angle of light emitted within the screen,  $\omega$ , to the angle of the light escaping the screen,  $\theta$ , by Snell's law. The normalized radiance of the emitted light at angle  $\theta$  to the normal is now given by

$$L(\theta)/L(0) = T_{n_p, n_c}(\omega) [(1 - e^{-k_p t_p / \cos(\omega)}) / (1 - e^{-k_p t_p})] \cos(\omega) \tag{3}$$

where  $n_p$  is the refractive index of the phosphor screen binder material and overcoat,  $n_c$  is the refractive index of the coupling medium between the screen and the lens or fibre optics, and  $\omega$  is the angle of emission prior to refraction. The transmission factor,  $T_{n_p, n_c}$ , at the overcoat-coupling medium interface is due to reflection of light back into the overcoat. This factor is given by Born and Wolf (1989) as

$$T_{n_p, n_c}(\omega) = \{ [n_c^2 - n_p^2 \sin^2(\omega)]^{1/2} / 2n_p \cos(\omega) \} \\ \times \{ [2n_c n_p \cos(\omega) / \{ n_c^2 \cos(\omega) + n_p [n_c^2 - n_p^2 \sin^2(\omega)]^{1/2} \}]^2 \\ + [2n_p \cos(\omega) / \{ n_p \cos(\omega) + [n_c^2 - n_p^2 \sin^2(\omega)]^{1/2} \}]^2 \}. \tag{4}$$

In the systems considered below, air ( $n_c = 1.0$ ) acts as the coupling medium for lenses, and optical coupling gel ( $n_c = 1.48$ ) is typically used with fibre optics.

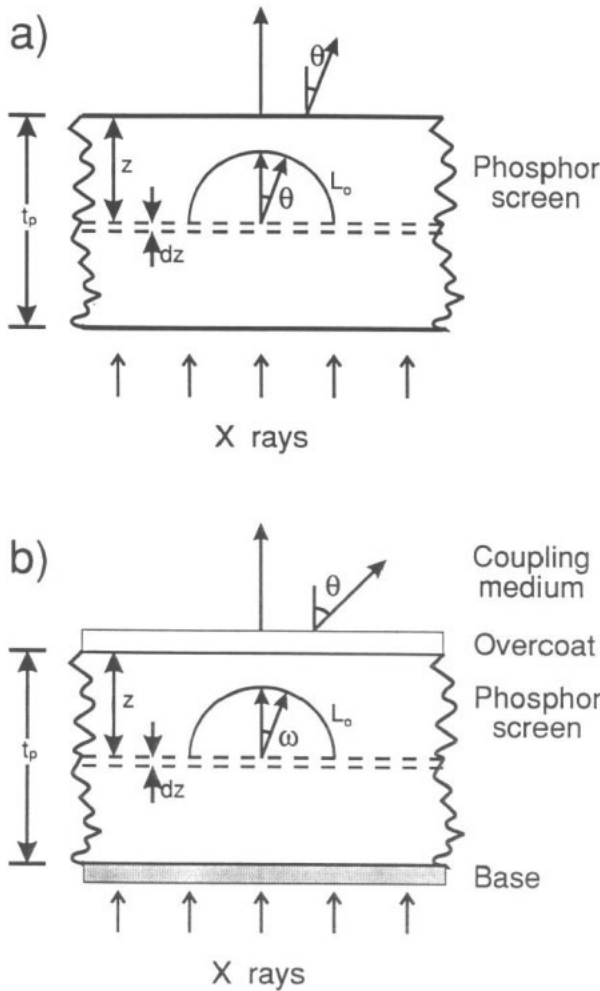


**Figure 4.** A schematic diagram of a phosphor illustrating (a) the angular emission model of Giakoumakis (equation (2)) and (b) our modified emission model for screens with a protective overcoat layer (equation (3)). In both models, the phosphor is divided into many layers of thickness  $dz$ , each of which is treated as a Lambertian light source. The light from the screen is the sum of the light from all such layers.

The mean angular distribution of light emitted from a single x-ray interaction is proportional to the radiant intensity of the light source,  $J(\theta)$ .  $J(\theta)$  is related to the radiance by  $J(\theta) = L(\theta) \cos(\theta)$ . Thus, the differential mean conversion gain of the phosphor screen may be expressed as a function of angle using

$$dg(\theta)/d\theta = g'(n_c) T_{n_p, n_c}(\omega) [(1 - e^{-k_p t_p / \cos(\omega)}) / (1 - e^{-k_p t_p})] \cos(\omega) \cos(\theta) \quad (5)$$

where  $g'(n_c)$  is a constant provided to ensure that the integral of  $dg(\theta)/d\theta$  over all values of  $\theta$  is equal to the total number of light quanta emitted from the screen.  $g'$  is expressed as a function of  $n_c$  to account for the dependence of the light output on the refractive index of the coupling medium. From these data, the total light output of the screen may be calculated.

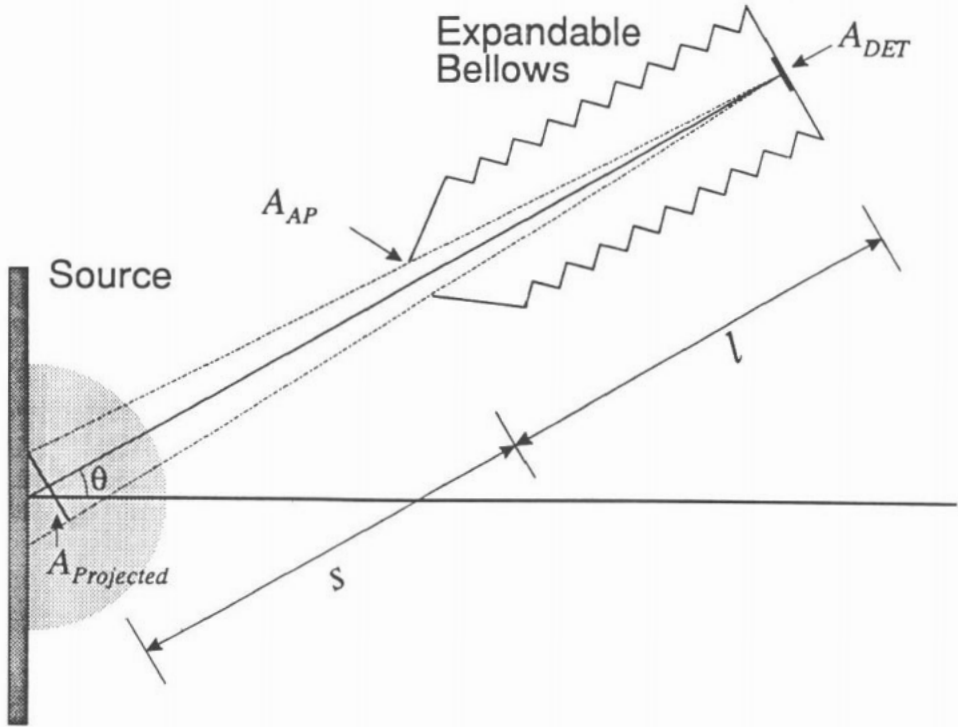


**Figure 5.** A schematic diagram of the goniometer used to measure angular-dependent radiance. The shaded semicircle denotes the position of an optional acrylic hemisphere used to measure the radiance of light emitted into a medium with a refractive index of 1.48.

### 3. Experimental procedure and results

A goniometer-mounted radiometer was constructed to measure the angular-dependent radiance of phosphor screens, and other light sources. The radiometer design (shown in figure 5) was based upon an expandable light-tight bellows. At the near end of the bellows, there is an aperture of area  $A_{ap}$ . At the far end of the bellows, a photomultiplier tube with an aperture of area  $A_{det}$ , is positioned. If the distance from the screen to the first aperture is  $s$ , and the distance from the first aperture to the second is  $l$ , then the projected area of the first aperture on the source,  $A_{projected}$  is  $A_{ap}(l+s)^2/l^2$ . The solid angle subtended by the detector,  $\Omega$ , is  $A_{det}/(l+s)^2$ . Therefore, the radiance of the light source,  $L(\theta)$ , is

$$L(\theta) = \Phi(\theta)/A_{projected}\Omega = \Phi(\theta)/A_{ap}A_{det}/l^2 \quad (6)$$

where  $\Phi(\theta)$  is the measured fluence at the detector (Boyd 1983). The radiant intensity,  $J(\theta)$ , is given by  $L(\theta) \cos(\theta)$ .

Table 1 lists the five phosphor screens evaluated. All of the screens were composed of  $Gd_2O_2S:Tb$  phosphor. Experiments were performed using 30 kV and 40 kV W target, constant-potential x-ray beams (HVL = 0.65 mm Al and 0.95 mm Al respectively), which are below the K edge energy of Gd. The radiance,  $L(\theta)$ , normalized to unity at  $\theta = 0^\circ$ , is shown in figure 6 for angles of  $\theta$  between  $0^\circ$  and  $70^\circ$ . The values of  $L(\theta)$  at  $\theta = 0^\circ$  relative

Table 1. Specifications of the phosphor screens examined.

Screen	Type	$k_p t_p$	Model	$L(0^\circ)$ relative to screen B at 30 kV	$L(0^\circ)$ relative to screen B at 40 kV
A	Min-R regular without overcoat	0.17	(2)	0.92	—
B	Min-R regular	0.60	(3)	1.00	1.00
C	Min-R medium	0.57	(3)	1.59	1.72
D	Lanex regular	0.72	(3)	2.68	3.27
E	Lanex medium	0.71	(3)	1.86	2.53

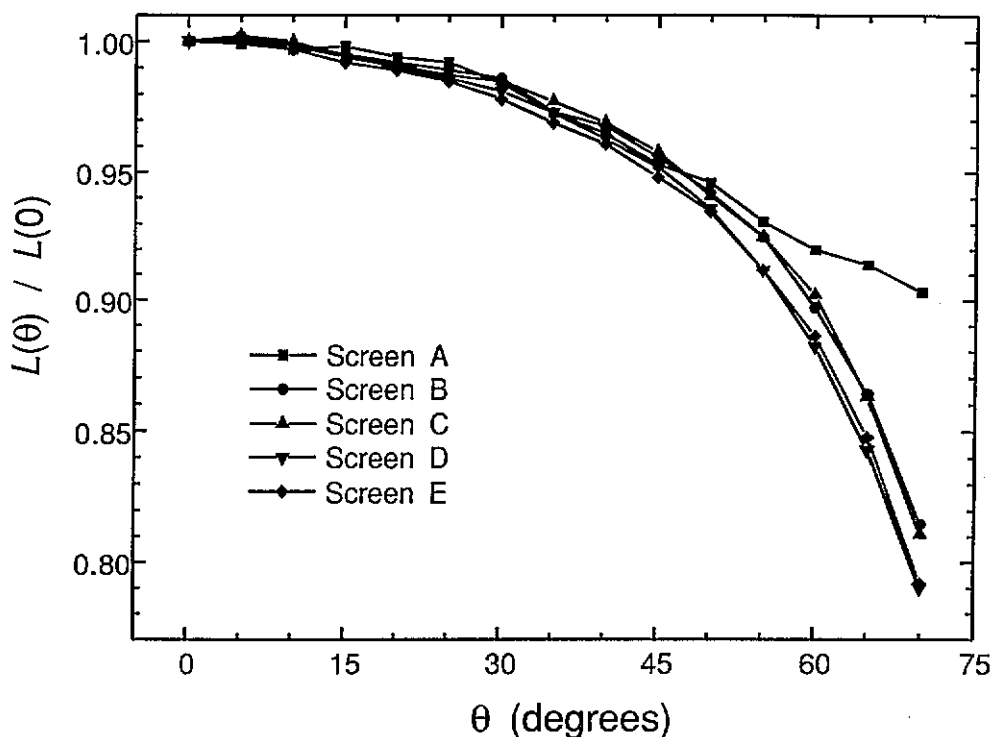


Figure 6. The measured angular-dependent radiance of light emitted from the five phosphor screens. The data have been normalized to unity at  $0^\circ$ .

to screen B are given in table 1. The apertures of the radiometer were  $A_{\text{det}} = A_{\text{ap}} = 2 \text{ mm}^2$ , with  $l = 15 \text{ cm}$  and  $s = 5 \text{ cm}$ . The goniometer and all surrounding surfaces were covered with black felt to avoid reflections. The measured results were symmetric about the central axis. Typically, the standard deviation in measured radiance was about 1%.

Phosphor screens B–E are commercially available for film–screen radiography. Screen A is similar to screen B, with the exception that the former lacks a protective overcoat layer. The angular emission data for screens B–E were fitted to equation (3) using a linear least-squares minimization, while the data for screen A were similarly fitted to equation (2). The fitted values of the product  $k_p t_p$  are given in table 1. Typically, the RMS deviation of the data from the fit was less than 0.5%.

Verification of the refraction from the overcoat to the coupling medium, and

quantification of the effect of the refractive index of the coupling medium on angular emission of light, were performed using screen B. First, the angular emission in air was measured as described above. To measure the angular emission in a denser medium (refractive index  $n = 1.48$ ), an acrylic hemisphere was coupled to the phosphor screen with an optical-coupling compound (Dow Corning #20-057,  $n = 1.48$ ), as shown by the shaded semicircle in figure 5. The x-rays incident at the centre of the 4 cm diameter hemisphere were collimated to a 1 mm diameter region to ensure that all light emitted from the screen would leave the hemisphere perpendicular to the surface. In this way, reflection losses were minimized and were independent of the angle of emission. The experimental results are shown in figure 7. The data acquired in the denser medium were fitted to equation (2) giving the product  $k_p t_p = 0.52 \pm 0.03$ , consistent with the value obtained with screen B in air using equation (3). Equation (4) and Snell's law were used to illustrate the effect of refraction of light from the dense coupling medium into air (shown in figure 7).

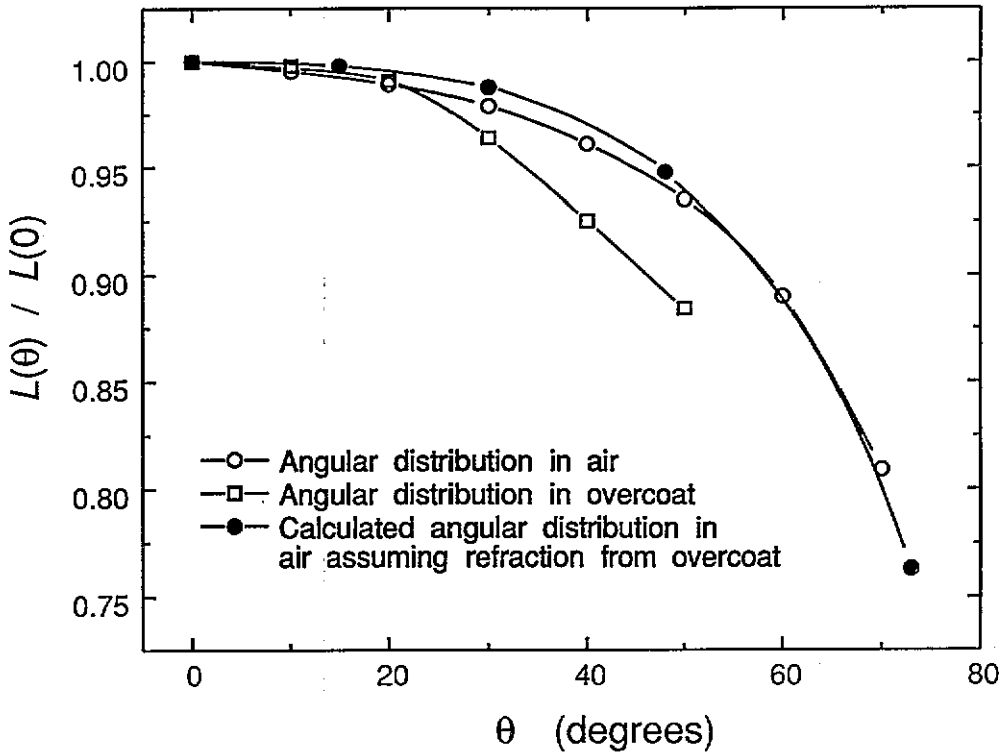
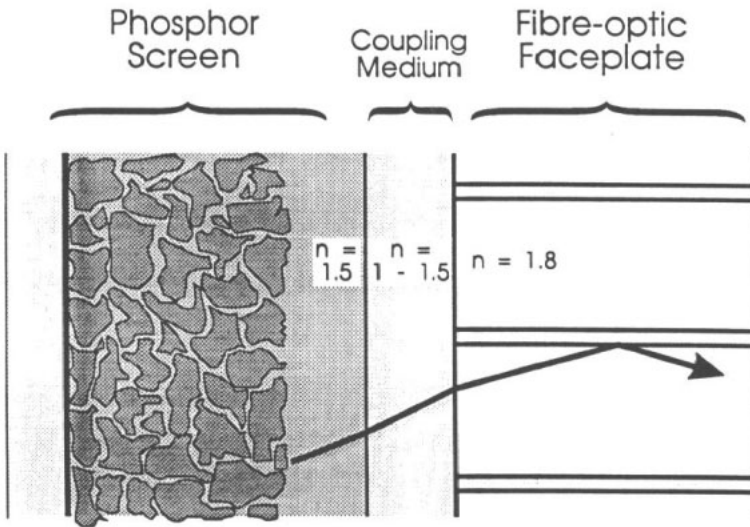


Figure 7. The measured angular emission of light from phosphor screen B in air (open circles) and in a medium with refractive index 1.48 (open squares). The effect of refraction from the overcoat into air was simulated using equation (4) and Snell's law.

Measurement of the light output of a phosphor screen as a function of the refractive index of coupling media is illustrated in figure 8(a). The measuring apparatus consisted of a CCD with a fibre optic window to which screen B was coupled using various media. The coupling media chosen were air ( $n = 1.0$ ), distilled water ( $n = 1.33$ ), and optical coupling

a)



b)

Relative Light Emission as a function of the refractive index of the coupling medium (Air = 1.0)

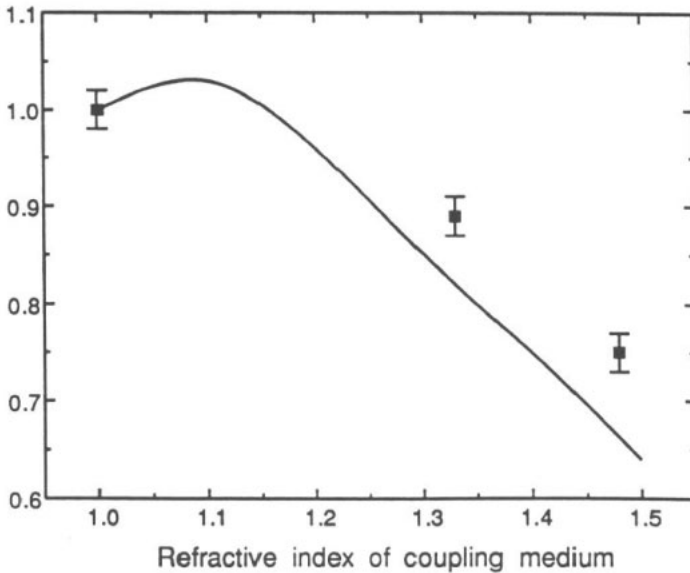


**Figure 8.** (a) A schematic diagram of an experiment to measure the relative light emission as a function of the refractive index of the coupling medium. In (b) the calculated and experimentally measured data demonstrate a reduction of light output with increased refractive index of the coupling medium. The experimentally measured data are shown using three different coupling media in conjunction with screen B.

gel ( $n = 1.48$ ). These media have refractive indices spanning the range of those that might be used in practice, while being inert with respect to the screen. For each coupling medium, the overall optical transmission was measured. These experimental results, shown in figure 8(b), are compared to predictions of our extended model (equation (3)), which accounts for the refraction of light in coupling the phosphor screen to the fibre optic and for the variation in the acceptance solid angle of the fibre optic as a function of the refractive index of the coupling medium.

#### 4. Discussion

A radiographic screen consists of a stiff plastic base upon which a scintillating phosphor material and a protective overcoat are added. Under microscopic examination, the phosphor layer is seen to consist of phosphor particles, coated and cemented together with a binder such as polyvinyl butyryl (Rabatin 1981). Because of the shape of the phosphor particles, the phosphor rarely occupies more than 50% of the total volume of the screen (Rabatin 1981, Barrett and Swindell 1981). The proportion of binder may be as little as 2% by weight to the phosphor (Degenhardt 1980). As a result, much of the volume is occupied by air cavities. Reducing the proportion of binder material produces an increase in spatial resolution (Degenhardt 1980), which is due to the increased scattering within the screen (Caruthers 1985, Roth *et al* 1979) caused by these cavities.

The protective overcoat is added to the screen to prevent the phosphor material of the screen from being damaged or eroded by the continual insertion and removal of films from the film-screen cassette. An overcoat also plays an important role in fibre-optically coupled POC digital mammography detectors when optical coupling compounds are used. These compounds are used to provide mechanical stability, optical alignment, and matching of refractive index. The overcoat material, being a continuous barrier, provides a necessary means of preventing the optical coupling compound from filling the interstices of air within the phosphor screen. We have observed that when these interstices are filled with coupling gel, the spatial resolution of the phosphor screen can be greatly degraded. We believe that this loss of resolution can be attributed to the same mechanism as observed by Degenhardt (1980).

Previous measurements of the angular emission of light from turbid phosphor screens (e.g., Giakoumakis and Miliotis 1985) have not considered the structure of commercial phosphor screens which include an overcoat material. As we have shown above, the overcoat material can markedly affect the optical properties and angular emission of light from such phosphor screens. Systematic discrepancies occurred between the model of Giakoumakis (equation (2)) and the measured values of angular emission of screens B-E, shown in figure 6. The key difference between the screens of Giakoumakis and our own was the existence of the overcoat material. To account for the overcoat material, we hypothesized that the interface between the overcoat and the coupling medium could be treated as being optically flat, and hence there would be refraction of the light at that interface. For example, in the case of the data shown in figure 6, the coupling medium was air, and refraction from the overcoat ( $n = 1.48$ ) to air would occur. The model given by equation (3), which accounts for this refraction, provides good agreement with the angular light emission data measured for screens B-E.

To verify the hypothesis of refraction, it was necessary to measure the angular distribution of light within the overcoat material. These data are presented in figure 7 for screen B. The measurement of the angular emission of light in air is redrawn from figure 6. As described above, the measurement of the angular emission of light in the overcoat was performed by coupling a hemisphere of equal refractive index to the overcoat to eliminate refraction in the air. To facilitate comparison of the two measurements, the effect of refraction into air was calculated based upon the angular emission of light in the overcoat. For example, light emitted at  $30^\circ$  to the normal in the overcoat would undergo refraction, and be emitted into air at  $48^\circ$ . Because of Fresnel reflective losses, given by equation (4), the intensity of the emitted light is reduced by 5.2%. The agreement between the calculated emission of light in air, and the measured emission data, supports our hypotheses that the overcoat is optically flat (to a first approximation) and that refraction occurs at the interface between the overcoat and the surrounding coupling medium.

These findings provide strong support for the underlying model proposed by Giakoumakis and Miliotis (1985). For example, we observed that the angular dependence of the emission of light was independent of the applied kilovoltage or HVL of the incident x-ray beam, while the relative intensities of the light produced from the screens did change. Both of these observations are in accordance with the model of Giakoumakis. Furthermore, two experiments were performed in which the phosphor screen design matched those of Giakoumakis: screen A (figure 6) and screen B coupled with gel to an acrylic hemisphere (figure 7). In both cases, all external sources of refraction and reflection had been eliminated, and in both cases accurate fits of the experimental data were made using equation (2). Note that the two experiments consisted of identical screens; however, one emitted light into air at the boundary of the phosphor layer, and the other emitted light into a medium of refractive index 1.48 at the boundary. Thus, although the phosphor thickness, dye additives, and backing materials are the same for screens A and B, the presence of the overcoat layer significantly affects the angular emission of light, as illustrated by the different values of  $k_p t_p$  listed in table 1. The difference between the values of  $k_p t_p$  in the two experiments is the result of the different probabilities of transmission of light from the phosphor binder into the exit medium. This effect can also be explained in terms of light diffusion models of phosphor screens (Klasens 1947). The coupling media will determine the boundary conditions of the diffusion equation, which governs the generation and propagation of light in the screen. Thus, changing the refractive index of the medium nearest to the phosphor screen has the effect of changing one of the boundary conditions for diffusion of light within the screen, but changing the refractive index of the medium in contact with the flat surface of the overcoat material only leads to refraction.

Figure 8 provides an illustration of the validity and the utility of the above results. The experimental apparatus, shown in figure 8(a), was used to determine the amount of light collected by a fibre optic faceplate when optically coupled to phosphor screen B. The data points in figure 8(b) were measured by altering the coupling material (air, water, and optical coupling compound). Similar results have also been observed with other screens. The curve in figure 8(b) is the result of calculations using equation (3) with  $k_p t_p = 0.52$ , and assuming the fibre optic has a 1.0 numerical aperture with the refractive index of the core glass being 1.78. This calculation included refraction from the phosphor overcoat to the coupling medium to the core glass, as well as the phosphor screen light emission and fibre optic light acceptance, which depends on the refractive index. The modelled data have been normalized to unity for a coupling medium of refractive index 1.0.

The modelled and measured data follow a similar trend. The discrepancies may be due, in part, to variations in the thickness of the various coupling media. Also, in equation (5), we expressed  $g'$  as a function of  $n_c$  because the refractive index of the coupling medium determines the probability of emission of light from the phosphor screen into the surrounding medium. This occurs, in part, because of self-attenuation of light in the phosphor screens. Before finally being emitted from a screen, a light quantum may have made several unsuccessful attempts at exiting the screen (Caruthers 1985, Roth *et al* 1979). If the probability of emission of light is reduced, then the probability of extinction of light prior to emission must increase. Even if emitted, the light quantum could be reflected back into the screen because of reflections at other interfaces. Thus, second-order effects of multiple reflections between the phosphor screen and the detector will affect the measured data. In this experiment, we have shown that the total number of light quanta does vary with the refractive index of the surrounding medium, and that this variation cannot be described by refraction and acceptance solid angle alone. Because the phosphor will act as a diffuse reflector, this process is difficult to model.

## 5. Conclusions

In summary, methods of calculating and measuring the angular emission of light from phosphor screens has been presented, and an analytic model of the angular emission of light from a phosphor screen was developed. The model was extended from the work of Giakoumakis and Miliotis (1985) to include turbid phosphor screens that possess a flat output surface due to the presence of a protective overcoat layer. This type of overcoat is common to all commercial radiographic phosphor screens. The model provided good agreement with measured angular emission data. The effect of refraction from the phosphor screen was demonstrated by measuring the angular emission of the light in the overcoat layer and in the coupling medium, each having different refractive indices.

We also measured the optical coupling efficiency of a fibre-optically coupled phosphor screen for which differing-refractive-index coupling media were used. It was shown that while light output increases with increasing refractive index of the optical coupling medium, the decreased acceptance angle of the fibre optic in fact reduces the overall coupling efficiency. Thus the greatest coupling efficiency occurs when a low-refractive-index coupling medium is used. Hence, we have shown that both the number and angular distribution of light quanta emitted from a phosphor screen is dependent on the refractive index of the coupling media.

## Acknowledgments

We gratefully acknowledge the assistance of Dr R Van Metter and Dr P Bunch of Eastman Kodak Research Laboratories, Rochester, New York, who provided the experiment screen (type A). This work was supported in part by the Medical Research Council of Canada, and the National Cancer Institute of Canada.

## References

- Barrett H H and Swindell W 1981 *Radiological Imaging* (New York: Academic) p 228
- Beerlage M J M, Levels H P L and Mulder H 1986 Digital slot radiography based on a linear x-ray image intensifier and two-dimensional image sensors *Proc. SPIE* 626 161-9
- Born M and Wolf E 1989 *Principles of Optics* 6th edn (New York: Pergamon) pp 38-42
- Boyd R W 1983 *Radiometry and the Detection of Optical Radiation* (New York: Wiley) pp 17-22
- Caruthers E 1985 Monte Carlo studies of image spread by x-ray intensifying screens *Proc. SPIE* 535 140-7
- Degenhardt H 1980 On the use of rare-earth luminescent materials in high-definition intensifying screens *Electromedica* 3 76-9
- Fritz S 1989 Scanned projection radiography using a time delay-and-integrate scanning CCD *Proc. SPIE* 1090 330-8
- Giakoumakis G E and Miliotis D M 1985 Light angular distribution of fluorescent screens excited by x-rays *Phys. Med. Biol.* 30 21-9
- Kapany N S 1955 Optical systems with flexible axes *PhD Dissertation* Imperial College, London
- Karellas A, Harris L J, Liu H, Davis M A and D'Orsi C J 1992 Charge-coupled device detector: performance considerations and potential for small-field mammographic imaging applications *Med. Phys.* 19 1015-23
- Klasens H A 1947 The light emission from fluorescent screens irradiated by x-rays *Philips Res. Rep.* 2 68-78
- Maidment A D A, Fahrig R and Yaffe M J 1993a Dynamic range requirements in digital mammography *Med. Phys.* 20 1621-33
- Maidment A D A and Yaffe M J 1994 Analysis of the spatial-frequency-dependent detective-quantum-efficiency of optically coupled digital mammography detectors *Med. Phys.* 21 721-9
- Maidment A D A, Yaffe M J, Plewes D B, Mawdsley G E, Soutar I C and Starkoski B G 1993b Imaging performance of a prototype scanned-slot digital mammography system *Proc. SPIE* 1896 93-103

- Nelson R S, Barbaric Z L, Gomes A S, Moler C L and Deckard M E 1982 An evaluation of a fluorescent screen-isocon camera system for x-ray imaging in radiology *Med. Phys.* **9** 777-83
- Rabatin J G 1981 Rare earth x-ray phosphors for medical radiography *Industrial Applications of Rare Earth Elements (American Chemical Society Symposium Series 164)* (Washington, DC: American Chemical Society) pp 203-18
- Roth B, Hamilton J F and Bunch P C 1979 Fundamental aspects of mammographic photoreceptors: screens *Reduced Dose Mammography* ed W W Logan and E P Muntz (New York: Masson) pp 529-36
- Sashin D, Gur D, Morris C W and Ricci J L 1976 Isocon imaging for x-ray diagnostics *Proc. SPIE* **78** 108-12